TEKA. COMMISSION OF MOTORIZATION AND ENERGETICS IN AGRICULTURE – 2014, Vol. 14, No. 4, 45–52

An Analysis of Pressure Distribution in Water and Water Emulsion In a Front Gap of a Hydrostatic Bearing

Konrad Kowalski, Tadeusz Zloto

Institute of Mechanical Technologies, Czestochowa University of Technology
Al. Armii Krajowej 21, 42-201 Czestochowa, konrad@itm.pcz.czest.pl, zlotot@o2.pl

Received December 05.2014; accepted December 18.2014

Summary. The paper presents pressure distributions for water and water emulsion in a variable-height gap of a hydrostatic thrust bearing with a rotating upper wall. On the basis of the Navier-Stokes equations and the continuity equation a formula is established for obtaining pressure in the gap. The paper also analyses the influence of geometrical parameters and exploitation conditions on the distribution of circumferential pressure around the smallest height of the gap.
Key words: pressure distribution**,** variable-height gap, hydrostatic thrust bearing, water, water emulsion.

INTRODUCTION

The problem of gap flow concerns a number of hydraulic devices and machines in which contact parts are separated by liquid-filled gaps of very small height. For gap flow of working liquids the Reynolds number is small and the flow is laminar [13, 26].

There are gaps of various shapes and dimensions. Since each gap in a hydraulic system is a source of loss [5, 6, 13, 21], it is important to examine phenomena that occur in them [14]. Losses are essentially dependent on the gap height: the greater the gap height the smaller the mechanical losses and the greater the volumetric losses [22].

Hydrostatic bearings are applied in popular hydrostatic drive systems [3, 4, 10, 16, 18, 19, 20]. In the case of axial pumps with a flat swash plate, a front gap can be found between slipper and swash plate and between cylinder block and valve. The smallest gap height between the slipper and swash plate is much greater than that between the cylinder block and valve plate [2]. The working liquid used in a hydraulic system is of crucial importance, too. The liquid is responsible for transferring large forces and torques of the system's elements. Selecting a working liquid has therefore economic and often environmental consequences.

Over the centuries, the discipline of fluid mechanics, including broadly conceived hydraulics, was developed by a number of prominent scientists, such as Thales of Miletus, Aristotle, Ktesibios, Archimedes, Da Vinci, Stevin, Torricelli, Pascal, Boyle, Newton, Bernoulli, Euler, Armstrong or Bramah [27]. In 1795, Bramah designed, patented and constructed the first hydraulic water press [11]. It was however observed that water as working liquid caused corrosion of metal elements and at the beginning of the 20th century American scientists Harvey Williams and Reynolds Janney came up with the idea of using mineral oil instead of water. They were the first to construct a hydrostatic piston axial gear with a swing swash plate [14]. This invention marks the beginning of the rapid development of oil hydraulics, which continues until today.

In hydraulic systems various liquids are used as working agents (Fig. 1). At present the one most frequently used is mineral oil [7, 23]. In places under the risk of fire, such as mines, non-flammable liquids are used.

The liquids applied are not perfect. With the multitude of industrial applications, it is necessary to search for liquids meeting the requirements as closely as possible.

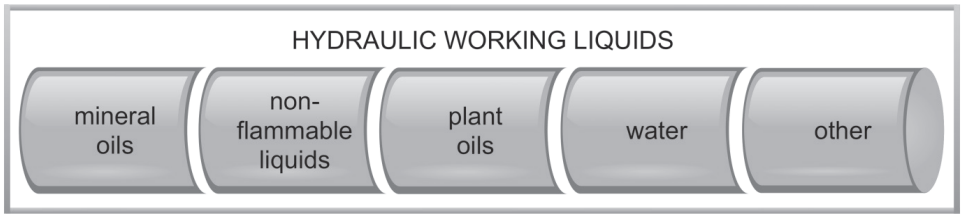

Fig. 1. Working liquids used in hydraulic drives

Because of that, studies are conducted on the application of plant oils in hydraulic systems. New opportunities seem to be offered by what is known as intelligent fluids, including electro-rheological and magneto-rheological fluids.

Besides, in the recent years there has been a revival of interest in water. Its applicability as a working agent in hydraulic systems is expected to rise due to the fact that it is environment-friendly and much cheaper than the other liquids currently used [11, 12, 17]. Following intensive research on water hydraulics [12], many producers and suppliers offer parts for modern water systems.

OBJECTIVES OF THE STUDY

The present study aims to examine the influence of exploitation parameters and dimensions on pressure distributions in the area surrounding the smallest height of the front gap in a hydrostatic thrust bearing with water and with a water emulsion. The study assumes an analytic model of pressure distribution in a front gap of the hydrostatic thrust bearing with a rotating upper wall.

A MODEL BASED ON THE NAVIER-STOKES EQUATIONS AND THE CONTINUITY EQUATION OF LIQUID PRESSURE DISTRIBUTION IN A FRONT GAP OF A HYDROSTATIC BEARING

Pressure distribution in the front gap of a hydrostatic thrust bearing (Fig. 2) can be best described analytically by means of a system of equations consisting of the Navier-Stokes equation and the continuity equation represented in a cylindrical system of coordinates r, φ, z [8, 15, 25]. A fluid element ABCDEFGH of dimensions dr, $rd\varphi$, dz is presented in Fig 3.

To solve the system of equations (1- 4) analytically, it is necessary to adopt the following simplifying assumptions:

- The gap is of micrometre high and is completely filled with incompressible liquid of constant viscosity;
- Surfaces are rigid;
- Liquid flow is laminar, uniform, steady and isothermal;
- Tangent stress is Newtonian;
- Liquid particles directly adjacent to the rotating wall surface have the same velocity as the rotating wall;
- Inertia is negligible.

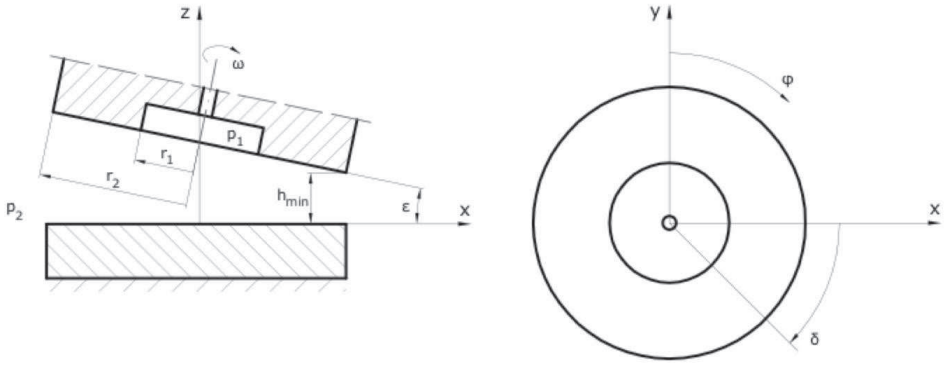

Fig. 2. Front gap of a hydrostatic thrust bearing [25]

The base system of equations is [8, 15, 25]:

$$\begin{cases} \dfrac{\partial v_r}{\partial t}+v_r\dfrac{\partial v_r}{\partial r}+\dfrac{v_\varphi}{r}\dfrac{\partial v_r}{\partial \varphi}+v_z\dfrac{\partial v_r}{\partial z}-\dfrac{v_\varphi^2}{r}= \\ =F_r+\nu\left(\dfrac{\partial^2 v_r}{\partial r^2}+\dfrac{1}{r}\dfrac{\partial v_r}{\partial r}+\dfrac{1}{r^2}\dfrac{\partial^2 v_r}{\partial \varphi^2}+\dfrac{\partial^2 v_r}{\partial z^2}-\dfrac{v_r}{r^2}-\dfrac{2}{r^2}\dfrac{\partial v_\varphi}{\partial \varphi}\right)-\dfrac{1}{\rho}\dfrac{\partial p}{\partial r}, \end{cases} \tag{1}$$

$$\begin{cases} \dfrac{\partial v_\varphi}{\partial t}+v_r\dfrac{\partial v_\varphi}{\partial r}+\dfrac{v_\varphi}{r}\dfrac{\partial v_\varphi}{\partial \varphi}+v_z\dfrac{\partial v_\varphi}{\partial z}+\dfrac{2v_r v_\varphi}{r}= \\ =F_\varphi+\nu\left(\dfrac{\partial^2 v_\varphi}{\partial r^2}+\dfrac{1}{r}\dfrac{\partial v_\varphi}{\partial r}+\dfrac{1}{r^2}\dfrac{\partial^2 v_\varphi}{\partial \varphi^2}+\dfrac{\partial^2 v_\varphi}{\partial z^2}+\dfrac{2}{r^2}\dfrac{\partial v_r}{\partial \varphi}-\dfrac{v_\varphi}{r^2}\right)-\dfrac{1}{\rho r}\dfrac{\partial p}{\partial \varphi}, \end{cases} \tag{2}$$

$$\begin{cases} \dfrac{\partial v_z}{\partial t}+v_r\dfrac{\partial v_z}{\partial r}+\dfrac{v_\varphi}{r}\dfrac{\partial v_z}{\partial \varphi}+v_z\dfrac{\partial v_z}{\partial z}= \\ =F_z+\nu\left(\dfrac{\partial^2 v_z}{\partial r^2}+\dfrac{1}{r}\dfrac{\partial v_z}{\partial r}+\dfrac{1}{r^2}\dfrac{\partial^2 v_z}{\partial \varphi^2}+\dfrac{\partial^2 v_z}{\partial z^2}\right)-\dfrac{1}{\rho}\dfrac{\partial p}{\partial z}, \end{cases} \tag{3}$$

$$\dfrac{\partial v_r}{\partial r}+\dfrac{1}{r}\dfrac{\partial v_\varphi}{\partial \varphi}+\dfrac{\partial v_z}{\partial z}+\dfrac{v_r}{r}=0. \tag{4}$$

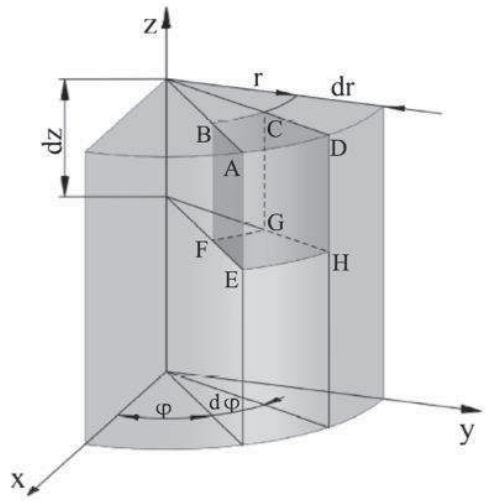

Fig. 3. A fluid element in a cylindrical coordinate system [1]

Besides, if $v_r = v_r(r, z)$ and $v_z = 0$, equations (1 - 4) become:

$$\begin{cases} 0=\nu\dfrac{\partial^2 v_r}{\partial z^2}-\dfrac{1}{\rho}\dfrac{\partial p}{\partial r}, & (5)\\ 0=\dfrac{\partial^2 v_\varphi}{\partial z^2}, & (6)\\ 0=\dfrac{\partial p}{\partial z}, & (7)\\ 0=\dfrac{\partial v_r}{\partial r}+\dfrac{1}{r}\dfrac{\partial v_\varphi}{\partial_\varphi}+\dfrac{v_r}{r}. & (8) \end{cases}$$

Equation (5) can be transformed and represented as:

$$\frac{\partial^2 v_r}{\partial z^2}=\frac{1}{\nu\rho}\frac{\partial p}{\partial r}. \tag{9}$$

To obtain the velocity v_r, it is necessary to integrate equation (9) twice with respect to the variable z. Then, the result is:

$$v_r=\frac{1}{2\nu\rho}\frac{\partial p}{\partial r}z^2+C_1z+C_2. \tag{10}$$

The integration constants C_1 and C_2 were obtained for the boundary conditions presented in Table 1.

Table 1. Boundary conditions for computing the integration constants C_1 and C_2

	No.	*Variable z*	*Velocity* v_r
Boundary conditions	*1.*	z = 0	$v_r = 0$
	2.	z = h	$v_r = 0$

Then, it follows:

$$C_1=-\frac{1}{2\nu\rho}\frac{\partial p}{\partial r}h, \tag{11}$$

$$C_2=0, \tag{12}$$

and after substituting (11) and (12) into equation (10):

$$v_r=\frac{1}{2\nu\rho}\frac{\partial p}{\partial r}(z^2-hz). \tag{13}$$

After integrating equation (6) twice with respect to the variable z, the velocity v_φ was obtained:

$$v_\varphi=C_3z+C_4. \tag{14}$$

The boundary conditions used for computing the integration constants C_3 and C_4 are presented in Table 2.

Table 2. Boundary conditions for computing the integration constants C_3 and C_4

	No.	*Variable z*	*Velocity* v_φ
Boundary conditions	*1.*	z = 0	$v_\varphi = 0$
	2.	z = h	$v_\varphi = \omega r$

Hence:

$$C_3=\frac{\omega r}{h}, \tag{15}$$

$$C_4=0, \tag{16}$$

and after substituting (15) and (16) into equation (14):

$$v_\varphi=\frac{\omega r}{h}z. \tag{17}$$

When (14) and (17) are substituted into (8):

$$0=\frac{1}{2\nu\rho}\frac{\partial^2 p}{\partial r^2}(z^2-hz)-\omega z\frac{1}{h^2}\frac{dh}{d\varphi}+\frac{1}{2\nu\rho r}\frac{\partial p}{\partial r}(z^2-hz). \tag{18}$$

Integrating equation (18) with respect to the variable z in the interval from 0 to h and performing some transformations yields:

$$\frac{\partial}{\partial r}\left(r\frac{\partial p}{\partial r}\right)=-6\nu\rho\omega r\frac{1}{h^3}\frac{dh}{d\varphi}. \tag{19}$$

To obtain a formula describing the pressure p in a front gap, it is necessary to integrate equation (19) twice with respect to the variable r. This leads to:

$$p=-\frac{3}{2}\nu\rho\omega r^2\frac{1}{h^3}\frac{dh}{d\varphi}+C_5\ln r+C_6. \tag{20}$$

The integration constants C_5 and C_6 were computed for the boundary conditions specified in Table 3.

Table 3. Boundary conditions for computing integration constants C_5 and C_6

	No.	*Radius r*	*Pressure* p
Boundary conditions	*1.*	$r = r_1$	$p = p_1$
	2.	$r = r_2$	p = 0

Hence:

$$C_5=\frac{3}{2}\nu\rho\omega\frac{1}{\ln\frac{r_2}{r_1}}\frac{1}{h^3}\frac{dh}{d\varphi}(r_2^2-r_1^2)-\frac{p_1}{\ln\frac{r_2}{r_1}}\cdot \quad (21)$$

$$C_6=\frac{3}{2}\nu\rho\omega r_2^2\frac{1}{h^3}\frac{dh}{d\varphi}-\frac{3}{2}\nu\rho\omega\frac{\ln r_2}{\ln\frac{r_2}{r_1}}\frac{1}{h^3}\frac{dh}{d\varphi}(r_2^2-r_1^2)+\frac{p_1\ln r_2}{\ln\frac{r_2}{r_1}}\cdot \quad (22)$$

Substituting integration constants (21, 22) into equation (20) ultimately leads to

$$p=\frac{3}{2}\nu\rho\omega\frac{1}{\ln\frac{r_2}{r_1}}\frac{1}{h^3}\frac{dh}{d\varphi}\left[(r_2^2-r^2)\ln\frac{r_2}{r_1}-(r_2^2-r_1^2)\ln\frac{r_2}{r}\right]+p_1\frac{\ln\frac{r_2}{r}}{\ln\frac{r_2}{r_1}}\cdot \quad (23)$$

RESULTS OF SIMULATIONS OF PRESSURE DISTRIBUTION IN THE FRONT GAP OF A HYDROSTATIC BEARING – AN ANALYSIS

Pressure was calculated in the front gap of a hydrostatic thrust bearing with water and with water emulsion AQUACENT LT 68. The basic physical parameters of these working liquids are presented in Table 4.

Table 4. Parameters of the working liquids

Parameter	Unit	Liquid	
		water	*water emulsion*
density	kg/m^3	988,1	930
kinematic viscosity	mm^2/s	0,548	68
water contents	%	100	41

The following input data were assumed in the computational model:

- Compression pressure p_1 = 20 Mpa,
- The smallest front gap height $h_{min} = 0.6\cdot10^{-6}$ m in the hydrostatic thrust bearing,
- Inclination angle of the upper wall with respect to the lower one $\varepsilon = 0.02°$,
- Angular velocity of the upper wall ω = 150 rad/s,
- Ratio of the external radius to the internal radius of the hydrostatic bearing $r_2/r_1 = 3$.

The height h of the front gap was obtained from the following formula [24]:

$$h=-r\sin\varphi\cos\delta\tan\varepsilon-r\cos\varphi\sin\delta\tan\varepsilon+r_2\tan\varepsilon+h_{min}, \quad (24)$$

where:

- r — any radius within the plane of the point u consideration,
- φ — current rotation angle,
- δ — angle measured with respect to the horizontal a for this angle the height of the front gap is smallest (in the xy plane).

In variable-height gaps there are two zones near the point of the smallest height: the confusor zone and the diffuser zone. In the confusor zone the gap height decreases along the gap and overpressure occurs. In the diffuser zone, on the other hand, the gap height increases along the gap and negative pressure occurs, which is partly limited by the cavitation phenomenon [9]. An example of pressure distribution for water and the radius r = 0.011 [m] near the smallest height point in a hydrostatic bearing is presented in Fig. 4.

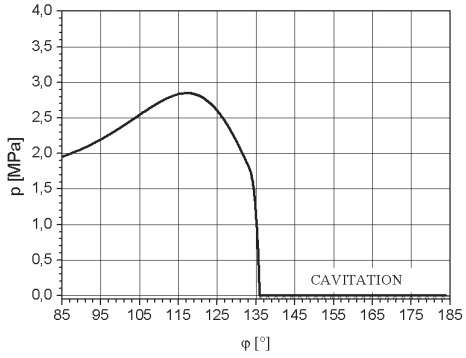

Fig. 4. Circumferential pressure distribution of water near the smallest-height point at the radius r = 0.011 m

A key parameter affecting the pressure of working liquids in a front gap is the kinematic viscosity factor. This can be seen very clearly in Fig. 5, where the values of the circumferential pressure in the hydrostatic bearing front gap are presented for water (ν=0.548 mm^2/s, ρ=988.1 kg/m^3) and for water emulsion AQUACENT LT 68 (ν=68 mm^2/s, ρ=930 kg/m^3), i.e. for working liquids which differ significantly with respect to kinematic viscosity. It can be observed that the values of the circumferential pressure increase as the viscosity of the working liquid increases.

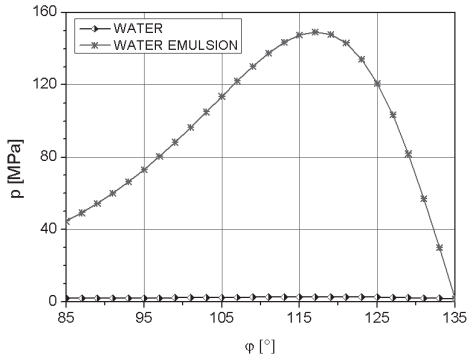

Fig. 5. Circumferential pressure distribution of water and water emulsion near the smallest-height point at the radius r = 0.011 m

In the interest of readability, in the graphs presented below different scales are used on the vertical axis for water and for water emulsion.

Fig. 6 presents circumferential pressure of water (Fig. 6a) and of water emulsion (Fig. 6b) in a confusor-shaped gap of the hydrostatic bearing for various minimal gap heights. The overpressure peaks occurring in the gap are the greater, the smaller the gap is.

Fig. 7 presents circumferential pressure of water (Fig. 7a) and water emulsion (Fig. 7b) in a front gap of the hydrostatic thrust bearing depending on the angle ε of the upper wall inclination. The pressure drops in the gap with increase in the angle ε.

Fig. 8 presents circumferential pressure of water (Fig. 8a) in a front gap of the hydrostatic thrust bearing and of water emulsion (Fig. 8b) depending on the angular velocity of the bearing upper wall. Here the pressure increases with increase in the angular velocity of the upper wall.

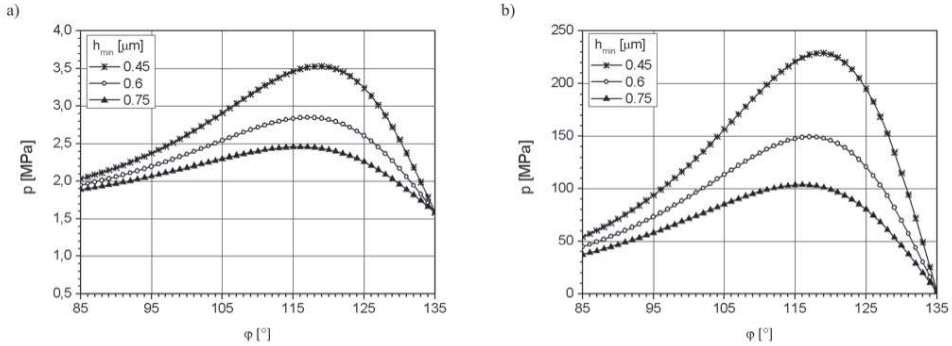

Fig. 6. Circumferential pressure distributions at the radius r = 0.011 m in a front gap for various values of the smallest gap height h_{min} for a) water, b) water emulsion

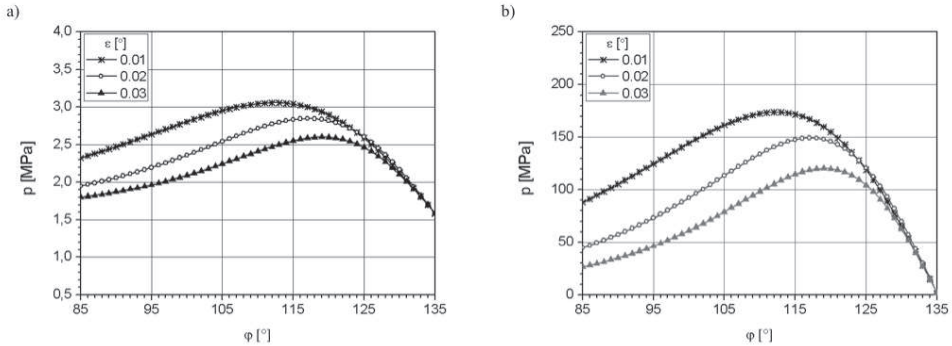

Fig. 7. Circumferential pressure distributions at the radius r = 0.011 m in a front gap for various values of the upper wall inclination angle ε for a) water, b) water emulsion

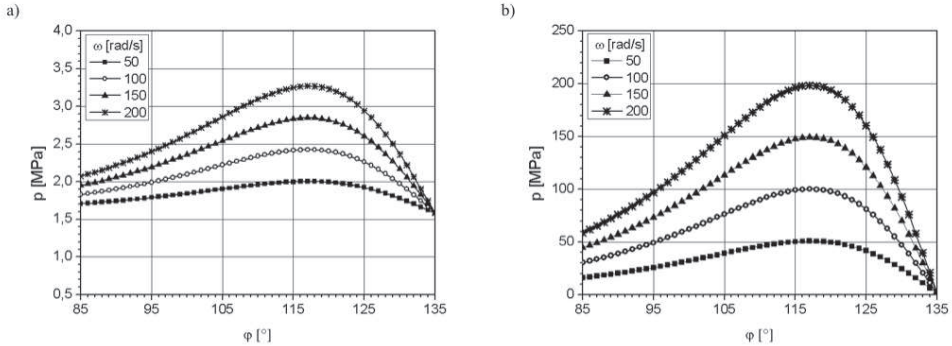

Fig. 8. Circumferential pressure distributions at the radius r = 0.011 m in a front gap for various values of the angular velocity ω of the upper wall for a) water, b) water emulsion

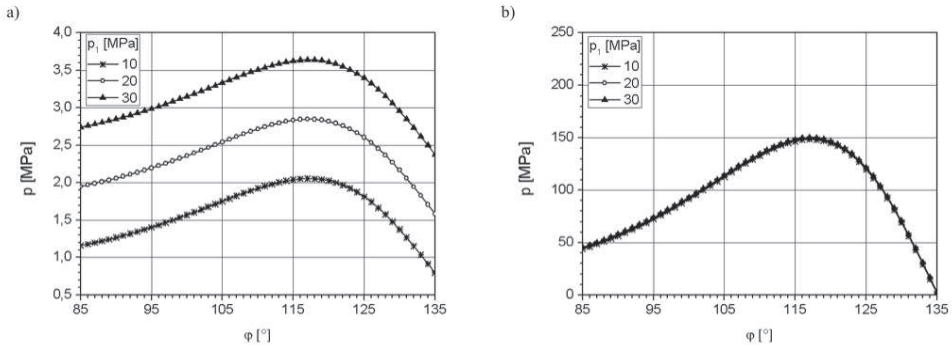

Fig. 9. Circumferential pressure distributions at the radius r = 0.011 m in a front gap for various values of the feeding pressure p_1 of the hydrostatic bearing for a) water, b) water emulsion

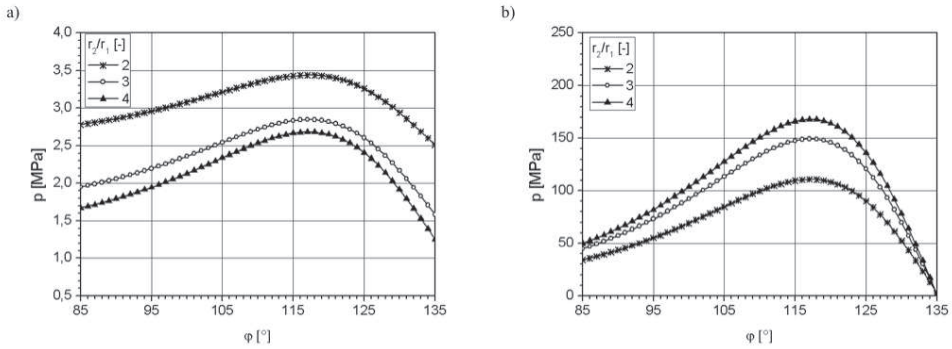

Fig. 10. Circumferential pressure distributions at the radius r = 0.011 m in a front gap for various dimensions of the hydrostatic bearing for: a) water, b) water emulsion

In the case of hydrostatic bearing with water as working liquid, the circumferential pressure in a front gap is significantly affected by the feeding pressure of the bearing. As the feeding pressure grows, the circumferential pressure grows, too (Fig. 9 a). For water emulsion, however, the influence of the feeding pressure is negligible (Fig. 9 b).

The value of the circumferential pressure depends also to a large extent on the dimensions of the hydrostatic bearing. Fig. 10 presents the circumferential pressure of water (Fig. 10a) and of water emulsion (Fig. 10b) in a front gap depending on the ratio of the external radius to the internal radius of the bearing. More specifically, in this study the external radius r_2 was assumed to be constant and only the internal radius r_1 varied to alter the size of the feeding chamber. For water, as the radius of the feeding chamber increases (so that the ratio r_2/r_1 decreases), the pressure grows in the gap. For water emulsion the opposite occurs: the greater the ratio r_2/r_1, the greater the value of the pressure in the gap.

CONCLUSIONS

The analyses presented above lead to the following conclusions:

1. The computational model adopted in the study is suitable for determining liquid pressure distribution in a front gap of a hydrostatic bearing with a rotating upper wall.
2. In the confusor zone near the smallest-height point the circumferential pressure increases. Its value depends on the dimensions and exploitation parameters of the bearing.
3. The pressure is higher for water emulsion than for water due to higher viscosity of the former.
4. In the confusor zone of the front gap there is an additional relief of the bearing caused by pressure increase.

REFERENCES

1. **Czetwertyński E., 1958:** Hydraulika i hydromechanika. PWN, Warszawa.
2. **Exner H. i in., Kempf H. (opracowanie i redakcja), Mecner W. (tłumaczenie) 2007:** Hydraulika. Podstawy, elementy konstrukcyjne i podzespoły. Vademecum hydrauliki, Tom 1, Wydanie 3 poprawione. Bosch Rexroth Sp. z o.o., Polska.
3. **Greczanik T., Stryczek J. 2005:** The concept of the bus fluid power system of the mining machine. Polska Akademia Nauk, Teka Komisji Motoryzacji i Energetyki Rolnictwa, Tom V, 72-79, Lublin.
4. **Hama T., Kurisu K., Matsushima K., Fujimoto H., Takuda H. 2009:** Outflow Characteristics of a Pressure Medium during Sheet Hydroforming, ISIJ International, Vol. 49, Nr. 2, 239-246.

5. **Ivantysyn J., Ivantysynova M. 2001:** Hydrostatic Pumps and Motors. Academia Books International, New Delhi.
6. **Ivantysynova M. 2008:** Innovations in pump design – What are future directions? Symposium on Fluid Power, JFPS, 59-64, Toyama.
7. **Klarecki K. 2012:** Eksploatacja układów hydraulicznych – oleje hydrauliczne. Utrzymanie Ruchu, Wydawnictwo Elamed, Nr 3, 6-8, Katowice.
8. **Kondakow L. A. 1975:** Uszczelnienia układów hydraulicznych. WNT, Warszawa.
9. **Kunze T., Brunner H. 1996:** Vibroakustische und optische Untersuchung der Kavitation bei Axialkolbenmaschinen. Ölhydraulik und Pneumatik, Nr 8, 542-546.
10. **Lasaar R. 2000:** The Influence of the Microscopic and Macroscopic Gap Geometry on the Energy Dissipation in the Lubricating Gaps of Displacement Machines. Proc. Of 1-st FPNI-PhD Symposium, Hamburg.
11. **Lim G.H., Chua P.S.K, He Y.B. 2003:** Modern water hydraulics – the new energy-transmission technology in fluid power. Applied Energy, Vol. 76, 239-246.
12. **Majdič F., Pezdirnik J., Kalin M. 2011:** Experimental validation of the lifetime performance of a proportional 4/3 hydraulic valve operating in water. Tribology International, Vol. 44, 2013-2021.
13. **Nikitin G.A. 1982:** Szczielewyje i łabiryntnyje upłotnienia gidroagregatow. Maszinostrojenie, Moskwa.
14. **Osiecki A. 2004:** Hydrostatyczny napęd maszyn. WNT, Warszawa.
15. **Osipow A. F. 1966:** Objemnyje gidrowliczieskie masziny. Maszinostrojenie, Moskwa.
16. **Osman T.A., Dorid M., Safar Z.S., Mokhtar M.O.A. 1996:** Experimental assessment of hydrostatic thrust bearing performance. Tribology International, Vol. 29, Nr 3, 233-239.
17. **Rokala M., Calonius O., Koskinen Kari T., Pietola M. 2008:** Study of lubrication conditions in slipper-swashplate contact in water hydraulic axial piston pump test rig. Proceedings of the 7th JFPS International Symposium on Fluid Power, TOYAMA 2008, 91-94.
18. **Ryzhakov A., Nikolenko I., Dreszer K. 2009:** Selection of discretely adjustable pump parameters for hydraulic drives of mobile equipment. Polska Akademia Nauk, Teka Komisji Motoryzacji i Energetyki Rolnictwa, Tom IX, 267-276, Lublin.
19. **Sasaki T., Mori H., Hirai A. 1959:** Theoretical Study of Hydrostatic Thrust Bearings. Bulletin of JSME, Vol. 2, Nr 5, 75-79.
20. **Sharma Satish C., Jain S.C., Bharuka D.K. 2002:** Influence of recess shape on the performance of a capillary compensated circular thrust pad hydrostatic bearing. Tribology International, Vol. 35, 347-356.
21. **Slanina F., Spałek J. 2007:** Analiza wpływu rodzaju cieczy roboczej pracującej w układzie hydraulicznycm na temperaturę i straty mocy. Szybkobieżne Pojazdy Gąsiennicowe Vol. 22, Nr 1, 99-104
22. **Stryczek S. 1984:** Napęd hydrostatyczny. Elementy i układy. WNT, Warszawa.
23. **Watton J. 2009:** Fundamentals of Fluid Power Control. Cambridge University Press, New York.
24. **Zloto T. 2009:** Modelling the pressure distribution in oil film in the variable height gap between the valve plate and cylinder block in the Arial piston pump. Polska Akademia Nauk, Teka Komisji Motoryzacji i Energetyki Rolnictwa, Vol. V, Nr 11, 418-430, Lublin.
25. **Zloto T., Kowalski K. 2012:** Pressure distributions in oil film in the front gap of a hydrostatic thrust bearing. Polish Academy of Sciences Branch in Lublin. Teka Commission of Motorization and Energetics in Agriculture, Vol. 12, Nr 2, 257-261, Lublin.
26. **Zloto T., Kowalski K. 2013:** Oil leaks intensity in variable-height gaps. Polish Academy of Sciences Branch in Lublin. Teka Commission of Motorization and Energetics in Agriculture, Vol. 13, Nr 2, 113-118, Lublin.
27. www.tiefenbach-waterhydraulics.com/waterhydraulics/historyofwaterhydraulics.html [dostęp: 22.07.2014]

ANALIZA ROZKŁADÓW CIŚNIENIA WODY I EMULSJI WODNEJ W SZCZELINIE CZOŁOWEJ ŁOŻYSKA HYDROSTATYCZNEGO

Streszczenie. W opracowaniu przedstawiono rozkłady ciśnienia wody i wybranej emulsji wodnej w szczelinie klinowej łożyska hydrostatycznego wzdłużnego z wirującą górną ścianką. W oparciu o równania Naviera-Stokesa i równanie ciągłości, określono zależność na wartości ciśnienia występującego w szczelinie. W pracy analizowano wpływ parametrów geometryczno-eksploatacyjnych łożyska hydrostatycznego wzdłużnego na rozkłady ciśnienia obwodowego w otoczeniu najmniejszej wysokości szczeliny.
Słowa kluczowe: rozkłady ciśnienia, szczelina klinowa, łożysko hydrostatyczne wzdłużne, woda, emulsja wodna.